Northumbria Research Link

Citation: Brahimi, Tahar, Khelifi, Fouad and Kacha, Abdellah (2021) An efficient JPEG-2000 based multimodal compression scheme. Multimedia Tools and Applications, 80 (14). pp. 21241-21260. ISSN 1380-7501

Published by: Springer

URL: https://doi.org/10.1007/s11042-021-10776-5 <https://doi.org/10.1007/s11042-021-10776-5>

This version was downloaded from Northumbria Research Link: http://nrl.northumbria.ac.uk/id/eprint/46419/

Northumbria University has developed Northumbria Research Link (NRL) to enable users to access the University's research output. Copyright © and moral rights for items on NRL are retained by the individual author(s) and/or other copyright owners. Single copies of full items can be reproduced, displayed or performed, and given to third parties in any format or medium for personal research or study, educational, or not-for-profit purposes without prior permission or charge, provided the authors, title and full bibliographic details are given, as well as a hyperlink and/or URL to the original metadata page. The content must not be changed in any way. Full items must not be sold commercially in any format or medium without formal permission of the copyright holder. The full policy is available online: http://nrl.northumbria.ac.uk/policies.html

This document may differ from the final, published version of the research and has been made available online in accordance with publisher policies. To read and/or cite from the published version of the research, please visit the publisher's website (a subscription may be required.)

Northumbria University NEWCASTLE

University Library

An efficient JPEG-2000 based Multimodal Compression Scheme

Tahar Brahimi[1], Fouad Khelifi[2] and Abdellah Kacha[3]
t.brahimi@gmail.com (t.brahimi@univ-jijel.dz), Fouad.khelifi@northumbria.ac.uk, akacha@ulb.ac.be

[1]L2EI Laboratory, Electronic Department, University of Mohammed Seddik Benyahia, BP 98, Jijel 18000, Algeria.

[2]Department of Computer and Sciences, Engineering and Environment, Northumbria University at Newcastle, United Kingdom.

[3]LPRA Laboratory, Electronic Department, University of Mohammed Seddik Benyahia, BP 98, Jijel 18000, Algeria.

Highlights

- This paper proposes a new efficient and fast multimodal compression technique.
- The idea relies on the combination of an ECG signal with the image in the wavelet domain prior to compression with a single codec (JPEG-2000).
- The proposed ECG signal insertion/extraction method makes the multimodal compression scheme more powerful than other competing techniques with less computational complexity.

Abstract

In this paper, a wavelet-based multimodal compression method is proposed. The method jointly compresses a medical image and an ECG signal within a single codec, i.e., JPEG-2000 in an effective and simple way. The multimodal scheme operates in two main stages: the first stage, consists of the encoder and involves a mixing function, aiming at inserting the samples of the signal in the image according to a predefined insertion pattern in the wavelet domain. The second stage represented by a separation function, consists of the extraction process of the ECG signal from the image after performing the decoding stage. Both the cubic spline and the median edge detection (MED) predictor have been adopted to conduct the interpolation process for estimating image pixels. Intensive experiments have been conducted to evaluate the performance of the multimodal scheme using objective distortion criteria. Results show clear superiority of the proposed scheme over the conventional separate compression approach involving two codecs: JPEG-2000 for images and ECG SPIHT-1D as well as other competing multimodal compression schemes in terms of both PRD and SNR at the signal decompression stage while maintaining good image quality and exhibiting a reduced computational complexity. Improvements in terms of average PRD and SNR values are as significant as 0.7 and 6 dB at low bit rates and 0.06 and 2 dB at higher bit rates on a number of test ECG signals and medical images.

Keywords: Multimodal signal-image compression, JPEG-2000 codec, SPIHT codec, Wavelet compression, Biomedical data compression

1. Introduction

The representation of constantly growing multimedia data (images, video, signal) in digital form optimizes their transmission through computer networks and facilitates their processing. Digitization, however, suffers from serious issues associated given the requirements on wide storage space and sufficiently large bandwidth. Compression, which aims to represent information in a compact form, thus appears to be the key not only to reduce storage space but also to ensure a rapid and efficient transmission of data [1-2].

With such a huge amount of ECG databases and growing demand of bandwidth, biomedical data (medical images, ECG, EEG, …) compression serves as a useful tool to help the processing for telemedicine applications including data sharing, monitoring, medical system control and so on. [3-6].

Based on the published literature, the main focus of attention tends to develop the algorithms commonly used to compress a particular type of data. In fact, little attention has been paid to the compression of two types of data, by the aid of a single codec. For instance, transform-based image coders such as EZW [7], SPIHT [8], SPECK [9], JPEG-2000 [10], and JPEGXR [11] are designed specifically for the purpose of image compression. Back in the nineties, Shapiro proposed a multiresolution-based image coder in [7], referred to as EZW, that exploits similarities across different

wavelet subbands by creating and using the concept of coefficients significance testing in a parent-descendants tree structure. The main idea relies on the assumption that if a parent is found to be insignificant when compared to a bit-plane threshold, its descendants are likely to be insignificant too. Later, Amir and Pearlman developed this idea and proposed a fast and powerful technique, called SPIHT [8], that exploits the tree structure in a more effective way. A few years later, the authors in [9] build upon the SPIHT algorithm to design a different subband structure using a block partitioning algorithm, called SPECK, while keeping similar lists for processing the significant and insignificant coefficients. Over the same period, the JPEG-2000 image compression system was standardized . It also uses the wavelet transform and offers distinctive features such as an improved compression efficiency particularly for low bit-rate, lossless and lossy compression within a single bitstream, progressive transmission (in quality and/or in resolution), region-of-interest (ROI) coding, and robustness to error transmission [10]. The coding process of JPEG-2000 is achieved by means of a block-based coder called EBCOT (Embedded Block Coding with Optimized Truncation of the embedded bit-streams)[Taub00], of which its inherent computational complexity, showing high degree, is the main disadvantage. The JPEG XR standard [11] offers a convenient coding technology for a wide range of applications with high compression capability and significant additional capabilities such as high compression capability, lossless and lossy compression), with simple encoder and decoder implementation requirements. The main intended application of JPEG XR is the representation of continuous-tone still images such as photographic images. In addition, JPEG XR accepts a wide range of colour coding formats, supporting monochrome, RGB, CMYK and n-component coding, utilizing a variety of unsigned integer, fixed-point and floating-point decoded digital representations with different bit depths. A particular focus of the development is to provide support for upcoming High Dynamic Range (HDR) imaging applications.

On the other hand, many ECG data compression algorithms have also been proposed separately in the literature [12-16]. In [12], the authors proposed a mono-dimensional version of SPIHT to compress ECG signals in a lossy fashion by modifying the conventional SPIHT-2D which had gained widespread recognition for its notable success in the field of image coding [12]. In [14], the authors adopted a new method that combines the empirical mode decomposition (EMD) with the wavelet transform to compress ECG signals. The authors in [15] applied a different approach by using the adaptive Fourier decomposition (AFD) algorithm to ECG compression and then performing lossless compression and built-in data encryption using a symbol substitution (SS) technique. The authors claimed that the idea of AFD algorithm hybridized with the SS technique would be more suitable for compressing ECG signals as it achieves a highly linear and robust relationship between the percentage root mean square difference (PRD) and the compression ratio (CR). In [16], an ECG compression technique was proposed based on sparse representation using a set of ECG segments as natural basis. The authors have shown good performance for their algorithm when compared with other related coders.

To the best of our knowledge, very little research has been devoted to multimodal compression in which two types of data are jointly compressed simultaneously by using a single codec (eg. image-biosignal or video-biosignal compression). This would make a powerful and attractive tool in telemedicine applications in which multiple data types are normally acquired. The work proposed by Zeybek et al. [17] can be considered the first and pioneering attempt to jointly compress an image with a biosignal with one codec. This was also reported in [4] by the same authors. Compared to conventional image compression schemes, this multimodal approach includes two further stages of biosignal insertion/separation respectively during the encoding/decoding process. In addition to higher performance that is normally obtained when compared to separate signal/image compression, multimodal compression also exhibits less computational complexity as the process of coding/decoding is conducted by a single codec on a combined signal/image data. In [12], the authors, propose a new approach to compress jointly a medical image and a multichannel bio-signals in the spatial domain. The spatial mixing function that inserts samples in low-frequency regions, is defined using a set of operations, including down-sampling, interpolation, and quad-tree decomposition. In [5], an improved multimodal compression scheme that builds upon [17] was developed [5][6]. This scheme, which uses a spiral insertion function in the wavelet domain to enhance the combination of the signal and image prior to compression, develops a more powerful multimodal compression technique that outperforms previous works while maintaining a reduced amount of computational complexity by using the SPIHT codec.

In this paper, a new multimodal compression method is proposed. The proposed method, based on the standard JPEG-2000, performs the wavelet transform for both image and signal, along with the use of the cubic spline interpolation or the MED predictor to estimate the substituted value of image pixels. Comparisons of performance with the conventional compression technique that employs two separate codecs to perform the compression of an image and a signal independently, are provided using the same test data. To make a fair comparison, the first codec of the conventional compression technique uses the standard JPEG-2000 for compressing the image apart taken, in accordance with the codec required of the multimodal scheme. The second codec, specific to the one dimensional biosignal, is the most popular wavelet-based coder in the literature [12], which uses the SPIHT algorithm, to achieve the compression of the ECG signal. In comparison with the conventional compression technique, the proposed coding strategy shows superior performance in terms of both percentage of root mean square difference (PRD) and signal to noise ratio (SNR) against compression ratio, when compared to [10][12]. In addition, a good quality of reconstructed image can be ensured, comparable to JPEG-2000 when it is applied to image individually. The rest of this paper is structured as follows. The JPEG-2000 standard is briefly described in section 2. Then, the principle of multimodal compression is illustrated in section 3 including our contribution. Section 4 presents the results obtained. Section 5 concludes this paper.

2.The JPEG 2000 standard overview

JPEG-2000 is a modern image compression standard established by the Joint Photographic Experts Group (JPEG), part of the International Organization for Standardization (ISO).

While exhibiting state-of-the-art compression performance superior to existing standards, JPEG-2000 compression engine offers distinctive features utilizing wavelet transform such as an improved compression efficiency particularly for low bit-rate, continuous-tone and bi-level compression, lossless and lossy compression within a single bit-stream, progressive transmission (in quality and/or in resolution), region-of-interest (ROI) coding, open architecture, robustness to bit errors, and protective image security [19-21, 10]. Two types of wavelet are selected: The 9/7 Daubechies wavelet for lossy compression, and the reversible 5/3 wavelet, implemented in integer lifting scheme, in the case of lossless compression. The EBCOT algorithm (Block Truncation Coding with Optimal) developed by Taubman [19] [21-10] serve as a basis for performing the coding process.

The encoding procedure is as follows: The original image (and its components) are partitioned into rectangular tiles for independent coding. Arbitrary tile sizes are allowed. Image tiling is optional and without tiling, the entire image is considered as one tile. Each tile is wavelet decomposed into different resolution levels, which consist of subband coefficients that describe the frequency characteristics local areas of tile components, rather than the entire image component. The subband coefficients of tiles are quantized (by using uniform scalar quantization with dead-zone in part I and trellis coded quantization in part II) and divided into packets separation locations [20]. A packet separation location consist of three spatially consistent rectangles (one from each sub-band at a given level of resolution), each of which is divided into regular non-overlapping rectangles, called coded blocks, which serve as the input of the entropy coder. Independent coding is performed of each block. Furthermore, for each block a separate progressive bit-stream is generated. Code-blocks are then coded a bit-plane at a time starting from the most significant bit-plane to the least significant bit-plane [19-21]. During the encoding of the individual bit planes of the coefficients in a code block three coding passes are completed, namely the significance propagation, the magnitude refinement, and the cleanup pass [19-21]. The first pass is used to encode the coefficients found to be insignificant (with their sign) and possess at least one significant of its eight-connected neighbours. During the magnitude refinement pass, all coefficients that were already significant in the previous bit-plane are encoded. The final pass, which is the clean-up pass, allows to encode all remaining (insignificant) coefficients. For each pass a context arithmetic coder is used to generate a compressed bit-stream of each code block. To overcome the drawback of coding independent code blocks where the redundancy around the code blocks in a sub-band (or among different sub-bands) is not exploited, the bit-streams from each code block are

organized so as to optimize the final bit-sream in terms of rate/distortion by using an algorithm named PCRD-opt (Post-Compression Rate-Distortion Optimization) [10].

3. Multimodal compression and the wavelet transform

The idea of multimodal compression scheme is to find favour of compressing jointly various data, of different modalities within a single coder. We can cite as an example the compression of an ECG signal with a medical image or video. In its abbreviated version, some pixels of the image are adequately replaced by samples of signal according to a function of mixture, thus providing data of mixture. This mixture is compressed using a given encoder. Then, this process is reversed by decoding the mixture, and then separating the signal from the image with the help of a separation function. Fig. 1 illustrates the essential steps of the multimodal image-signal compression process [4][6].

Multimodal compression methods can be classified into 2 categories, according to the insertion process: non-supervised multimodal compression methods and supervised multimodal compression methods.

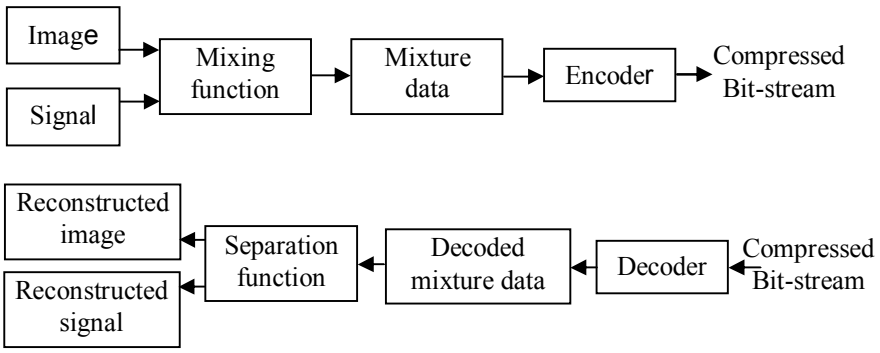

Fig. 1 Block diagram representing the principle of multimodal image-signal compression

With regards to non-supervised multimodal compression method, the insertion process of the signal into the image is conducted without taking into account the frequency content of the image. On the contrary, in supervised multimodal compression methods, the insertion process relies on the analysis of the candidate region for inserting the signal in order to find the best insertion area. Indeed, the selected areas display a certain degree of homogeneity and do not include the sensitive regions that might affect the visual quality at reconstruction [22].

The wavelet transform has attracted an increasing body of research in a broad field of image processing applications including signal, image, and video compression [23-29]. As a result, wavelet-based image coding has proven to provide superior performance to those that use discrete cosine transform or spatial techniques [30-33]. To establish a lossless compression scheme based on the wavelet transform, the wavelet coefficients with integer values must be obtained so that quantization errors are avoided [34-38]. Therefore, the perfect reconstruction of the input signal can be performed. In the context of multimodal compression framework, which belong to the class of lossy compression schemes, the wavelet

transform was successfully applied to conduct the insertion process [17][4][6].The first multimodal compression using the wavelet transform was proposed in [17], and has been considered in a specific medical application. The signal is firstly modified by a scaling factor and inserted in the detail sub-band (HH) after achieving the DWT on the input image. The coding process occurs after performing the IDWT on the mixture data. Recently, an improved multimodal signal-image compression has been proposed based on the wavelet transform and on The Set Partitioning In Hierarchical Trees (SPIHT) codec, which is served as a basis for achieving the coding/decoding process.

3.1 Proposed multimodal compression scheme

The proposed multimodal compression scheme is a different variant of methods [17][6]. It is based on JPEG-2000 standard and conducts the insertion process in the wavelet domain. At first, the 2D and 1D discrete wavelet transform are performed respectively to the input image and quantized signal up to 6 and 4 decomposition levels respectively using the 9/7 biorthogonal filter.

For compressing colour images, a colour transformation based on a luminance chrominance representation is conducted instead of the common usage of RGB model in colour image acquisition and display. Because the multimodal scheme belongs to the class of lossy compression techniques, the lossy colour transformation (Ycbcr in our study) is used, and the insertion is performed on the luminance component Y.

According to a mixing function, the resulting 1D signal is inserted in a detail-subband of the wavelet decomposed image. The insertion area is decimated to comprise the signal samples to be inserted, similar in construction to [17] with the difference of quantization process of signal samples. Note that the signal quantization process necessarily leads to provide a dynamic range similar to that of the input image. Note that the method in [17] depends on a scaling factor of which a bad choice exerts real influence on compression performance.

Let us consider an insertion area, located at HH_1 subband, and defined by *(x,y)*, *w*, *h* as follows :

(x,y): the coordinates of the top left corner of the insertion area.

w, *h*: are respectively the width and the high of the insertion area.

The insertion process, roughly similar to [17], of the *ith* sample of the wavelet quantized signal, of length *N*, denoted as S_{wqi} is as follows:

$$HH_1(x' + 2k, y' + 2l) = S_{wqi} \qquad (1)$$

where:

$$x' = \left\lfloor \frac{x}{2} \right\rfloor, \quad y' = \left\lfloor \frac{y}{2} \right\rfloor, \quad w_1 = \frac{w}{2}, \quad h_1 = \frac{h}{2}$$

$$i = 0, \ldots N; \quad k = 0 : w_1 - 1 = 0 : \frac{w}{2} - 1; \quad l = 0 : h_1 - 1 = 0 : \frac{h}{2} - 1 \qquad (2)$$

and $\lfloor . \rfloor$ rounds the elements of x to the nearest integers towards minus infinity.

The extraction process of the *ith* sample of the decoded quantized ECG signal from the HH_1 subband, denoted as $\hat{S}_{wqi}$ is given by:

$$\hat{S}_{wqi} = HH_1(x' + 2k, y' + 2l) \qquad (3)$$

Note that the capacity of insertion in a given insertion area of size $(w \times h)$ does not exceed $(w \times h)/4$.

The mixture data are then coded by JPEG-2000. After performing the decoding process, a further stage of separation is performed to get decoded versions of image and signal. Lastly, the 2D and 1D inverse discrete wavelet transform are performed respectively to the decoded image and quantized signal. The process of image reconstruction necessarily involves a step of interpolation in order to restore the image pixels that have been replaced by signal samples. The Median Edge Detector (MED) predictor [39][40][17] is used to estimate the substituted value of image pixels in the first multimodal method. On the other hand, the second method uses the Cubic Spline interpolation. The block diagrams of the proposed multimodal scheme for both coding and decoding are illustrated respectively in Figs. 2 and 3.

The essential difference with method [6] lies in the fact that the insertion process is different from the spiral way preformed in [6], the encoder employed: The standard JPEG-2000 instead of SPIHT, and the way of estimating image pixels. Indeed, two different interpolation techniques are employed as previously reported. The difference from [17] lies in the way the mixture image is obtained, and the scaling process as previously mentioned. In [17], first a DWT of level 1 is performed, and then the signal is modified by a scaling factor and inserted into the detail sub-band (HH). Next, an IDWT is achieved to reconstruct the image mixture considered as the input image. Another DWT is also performed, generally up to level 6 during the coding process of JPEG-2000.

The pseudo code of the coding process is as follows:

1. Perform the 2D wavelet decomposition (up to level 6) using the 9/7 biorthogonal filter for the input image.
2. First apply the quantization process to the ECG signal , and then perform the 1D wavelet decomposition (up to level 4) using the 9/7 biorthogonal filter.
3. Conduct the insertion process of the quantized wavelet decomposed ECG signal in the HH_1 detail subband at the finest scale using equations (1) and (2).
4. Encode the mixture data (wavelet coefficients of image and ECG signal) using JPEG-2000 encoder.

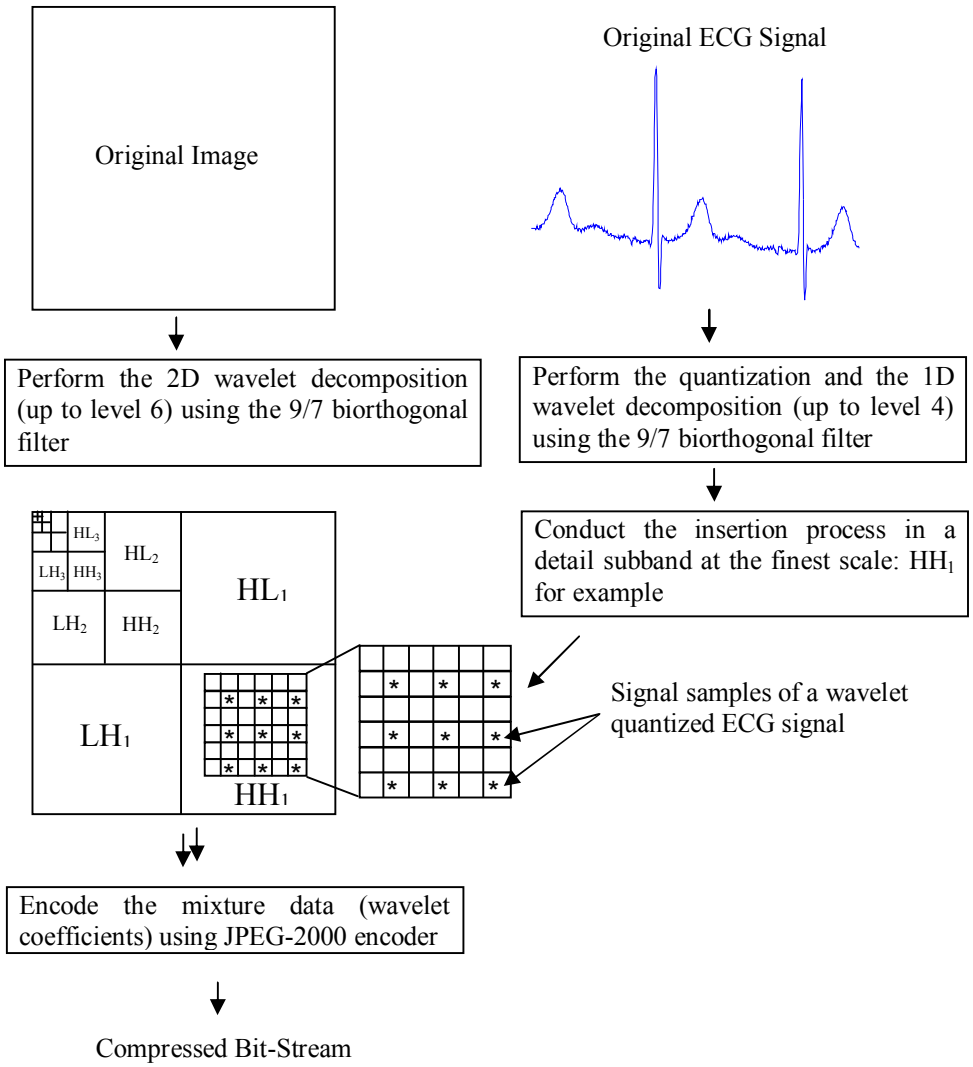

Fig. 2 Block diagram illustrating the encoding process of the proposed multimodal image-signal compression scheme using the standard JPEG-2000

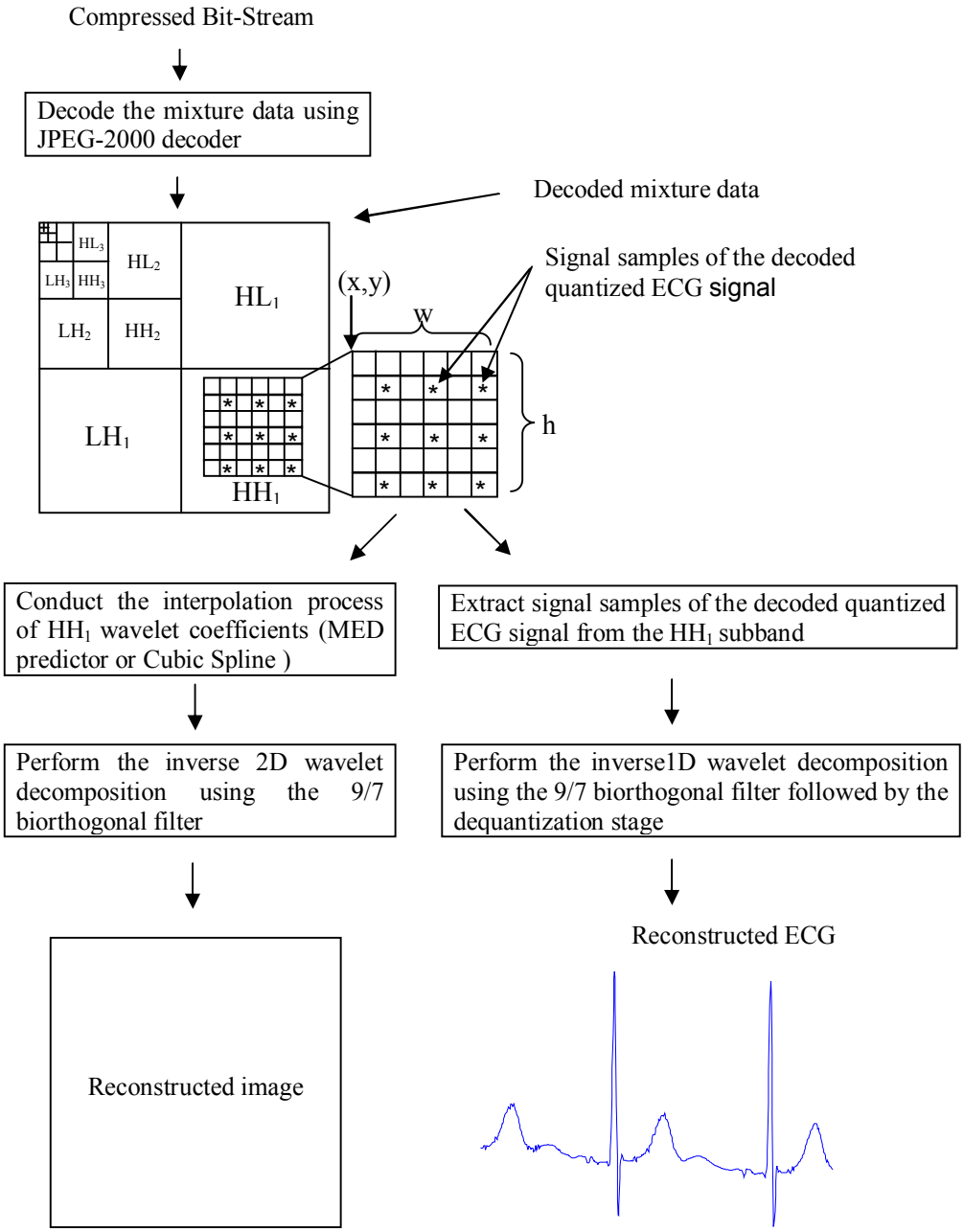

Fig. 3 Block diagram illustrating the decoding process of the proposed multimodal image-signal compression scheme using the standard JPEG-2000

4. Experimental results

To evaluate the effectiveness of the proposed multimodal compression scheme, the performance of five competing compression techniques are compared on the same images and ECG signals, namely: the proposed multimodal compression scheme namely: Multimodal scheme 1 (JPEG-2000 based multimodal compression scheme: Interpolation with cubic spline), the multimodal methods proposed in [17] [4] [6] , and the separate compression method involving the use of two codecs: JPEG-2000 for compressing the image [10] and SPIHT-1D for the compression of the ECG signal [12]. This is referred to as the separated JPEG-2000/SPIHT. To make our comparison as fair as possible, the multimodal methods as well as the image codec, required in the separated compression approach use the same codec, i.e., the standard JPEG-2000 with the same setting parameters in the compression phase such as the wavelet transform and the number of decomposition levels. In our experiments, 22 medical images of varying sizes (512 x 512 and 1024 x 1024) have been used. It is worth noting that the difference between multimodal scheme 1 and multimodal scheme 2 (JPEG-2000 based multimodal compression scheme: Interpolation with MED predictor) is minor and this does not really require the inclusion of both in experiments. The ECG data used here is the record 103b in MIT-BIH arrhythmia database. The record of length 16384 samples, is sampled at 360 Hz, and the resolution is 11 bits/sample. Among the mostly used distortion criteria for performance evaluation is the percent root mean square difference (PRD) , defined as [3] [12]:

$$PRD(\%) = \sqrt{\frac{\sum_{i=1}^{N}(x_i - y_i)^2}{\sum_{i=1}^{N}(x_i)^2}} \times 100 \qquad (4)$$

Where:

x_i is the original signal, y_i is the reconstructed signal. And N is the number of samples over which the PRD is calculated. In addition to PRD we also provide the values of SNR for measuring the distortion of the ECG signal after recovery. This is expressed as:

$$SNR(dB) = 10 \log_{10}\left(\frac{\sum_{i=1}^{N}(x_i)^2}{\sum_{i=1}^{N}(x_i - y_i)^2}\right) \qquad (5)$$

Note that in [3] the relation between PRD and SNR is established. For the image quality evaluation, the Peak Signal to Noise Ratio (PSNR) has been adopted and defined as follows:

$$PSNR = 10\log_{10}\frac{\left(2^{B}-1\right)^{2}}{MSE} \qquad (6)$$

where

$$MSE = \frac{1}{NM}\sum_{i=1}^{N}\sum_{j=1}^{M}\left(\mathrm{x}(i,j)-\mathrm{y}(i,j)\right)^{2} \qquad (7)$$

$\mathrm{x}(i,j)$ is the original image with dimensions $M \times N$ and having B bits/pixel. And $\mathrm{y}(i,j)$ is the reconstructed image.

The Structural SIMilarity (SSIM) index is also an improved method for measuring image quality for y given the reference image x [41]. It is based on the a multiplicative combination of the three terms, namely the luminance term, the contrast term and the structural term. The simplified version is as follows:

$$SSIM(x,y) = \frac{\left(2\mu_x\mu_y + C_1\right)\left(2\sigma_{xy} + C_2\right)}{\left(\mu_x^2 + \mu_y^2 + C_1\right)\left(\sigma_x^2 + \sigma_y^2 + C_2\right)} \qquad (8)$$

where $\mu_x, \mu_y, \sigma_x, \sigma_y$, and σ_{xy} denote the local means, standard deviations, and cross-covariance for images x and y.

$C_1 = \left(k_1 d\right)^2$ and $C_2 = \left(k_2 d\right)^2$ are two small positive constants necessary to stabilise the division.
d is the range of intensities. k_1=0.01, k_1=0.03 by default.

4.1 Performance comparison with the separated compression approach

We have assessed the performance of the proposed multimodal compression scheme against the separated approach using a set of 12 medical images of size 1024 x 1024 [42], and the record 103b from MIT-BIH arrhythmia database. Each image sample is quantified at 8 bits per pixel. Six and four levels of decomposition have been performed using the biorthogonal 9/7 filters for the image and the signal, respectively. Note that the performance evaluation process when compressing an image and a signal together should take into account three factors: the compression ratio (or bit rate), an image distortion measure and a signal distortion measure. At a given bit rate, an effective multimodal technique aims to achieve high values of PSNR (or SSIM) for image distortion evaluation, and, at the same time, offers low values of PRD (or high values of SNR) for ECG distortion measure.

In multimodal compression, it is meant by nbpp the bit rate calculated by using the image size but corresponding to the bits required to compress both the image and the ECG signal. Since the compressed image also includes the ECG signal, it is referred to as compressed multimodal image/signal. In the case of separated coding and in order to ensure that comparison is fair, the number of bits required to represent the compressed multimodal image/signal with nbpp is used to code both the image and the ECG signal separately. Table 1 compares performance obtained with the proposed

multimodal method as well as the separated compression approach at different nbpp values (0.125, 0.25, 0.5 and 0.75 bpp). As can be seen in Table 1, the quality of the decompressed ECG signal is clearly better for our proposed method when considering an equal number of bits for representing both the signal and image and a roughly similar visual quality of the reconstructed images. In fact, with the same (or very close) values of the PSNR or SSIM, the value of PRD is significantly lower and the SNR is considerably higher respectively. For example, for image 00000271_003 when the number of bits required to represent the compressed multimodal image/signal is 524288 bits which would correspond to a separate compression of the image and the signal at nbpp=0.5 bpp, the two methods have similar values of PSNR and SSIM (43.3720 dB, 0.7099). However, the PRD values with the proposed scheme are much smaller while and the gain in SNR reaches 1.7 dB, approximately. Note also that the gains for PRD and SNR values are especially more significant at low bit rates (number of bits <=262000 bits). In Fig.4, the average rate distortion is compared, taken over 12 test medical images at several bit rates in terms of PSNR, SSIM, PRD, and SNR. The average gains of PRD and SNR are also reported in Fig. 4 (e-f). It can be shown that the average PRD and SNR of the proposed method are the best at each bit rate, especially at lower bit rates for the same value (or very close) of PSNR and SSIM. This clearly shows the superiority of our proposed multimodal compression scheme over the separated approach. In Fig. 5 and 6, we provide respectively an example of the ECG and medical image reconstructions obtained at 798720 bits with the two methods. As illustrated in Fig. 5, The proposed method produces the highest performance, significantly improves the performance with a gain up to 0.20 and 10 dB respectively in terms of PRD and SNR. On average, the proposed method achieves a gain of [0.7-1.75] and [5-9.8]dB respectively in terms of PRD and SNR at low bit rates. The gain in SNR varies between 2 dB and 3 dB at higher bit rates, as shown in Fig. 4 (e-f).

4.2 Performance comparison with multimodal compression methods

To assess the performance of the proposed compression scheme in comparison with other competing multimodal compression schemes, experiments were carried out on 10 medical images of size 512 x 512, where each image sample is quantified at 8 bits per pixel). Performance results at several bit rates ranging from 0.25 bpp to 1 bpp are compared to those obtained with the multimodal compression methods reported in [4], and those obtained with its improved versions proposed in [17] [6]. Similar to previous experimental settings, six and four levels of the dyadic wavelet decomposition were applied to the image and signal, respectively using the biorthogonal 9/7 wavelet filters. The results obtained are reported in Table.2. As can be seen, results show that the proposed scheme performs significantly better that its competitors in terms of both signal and image quality at the same bit rate, while the method in [17] performs better than that of [4]. Given similar values of PSNR and SSIM, the PRD values are significantly lower and the SNR is consistently higher. If one takes the multimodal scheme [6] as a reference point, the proposed multimodal method

Table 1 Performance compression comparison of various coding methods. Separate compression method: the method which involves the use of two codecs in the compression process: JPEG-2000 for image, SPIHT-1D for ECG. Proposed multimodal scheme: JPEG-2000 based multimodal compression scheme: Interpolation with cubic spline

Medical image	Number of bits	Metric	Separated JPEG-2000 / SPIHT	Proposed multimodal scheme	Number of bits	Metric	Separated JPEG-2000 / SPIHT	Proposed multimodal scheme
00000271_004	131072	PSNR	39.7160	39.6664	524288	PSNR	43.6199	43.573
		SSIM	0.4926	0.4905		SSIM	0.6915	0.6904
		PRD	3.2837	**1.5432**		PRD	0.5564	**0.269**
		SNR	26.6728	**36.2315**		SNR	45.0926	**51.398**
	262144	PSNR	41.5717	41.5200	798720	PSNR	45.1914	45.173
		SSIM	0.5878	0.5855		SSIM	0.7586	0.7576
		PRD	1.6412	**0.5719**		PRD	0.2846	**0.236**
		SNR	35.6968	**44.8534**		SNR	50.9160	**52.557**
00000271_003	131072	PSNR	39.3243	39.2920	524288	PSNR	43.3720	43.3720
		SSIM	0.5077	0.5061		SSIM	0.7099	0.7099
		PRD	3.2837	**1.4536**		PRD	0.5564	**0.4609**
		SNR	26.6728	**36.7512**		SNR	45.0926	**46.7283**
	262144	PSNR	41.3085	41.3004	798720	PSNR	44.9811	44.9622
		SSIM	0.6068	0.6066		SSIM	0.7784	0.7755
		PRD	1.6412	**1.2230**		PRD	0.2846	**0.2429**
		SNR	35.6968	**38.2514**		SNR	50.9160	**52.2900**
00000271_001	131072	PSNR	43.5920	43.4786	524288	PSNR	49.3828	49.3622
		SSIM	0.4895	0.4853		SSIM	0.6405	0.6403
		PRD	3.2837	**1.4536**		PRD	0.5564	**0.4707**
		SNR	26.6728	**36.7512**		SNR	45.0926	**46.5456**
	262144	PSNR	46.5217	46.4941	798720	PSNR	50.9532	50.9316
		SSIM	0.5629	0.5621		SSIM	0.7016	0.7015
		PRD	1.6412	**1.1005**		PRD	0.2846	**0.0882**
		SNR	35.6968	**39.1685**		SNR	50.9160	**61.0953**
00000271_002	131072	PSNR	42.0979	41.9478	524288	PSNR	48.3330	48.2275
		SSIM	0.5089	0.5032		SSIM	0.7096	0.7094
		PRD	3.2837	**1.4536**		PRD	0.5564	**0.4707**
		SNR	26.6728	**36.7512**		SNR	45.0926	**46.5456**
	262144	PSNR	45.3100	45.2222	798720	PSNR	50.1914	50.0038
		SSIM	0.6111	0.6098		SSIM	0.7768	0.77
		PRD	1.6412	**1.1005**		PRD	0.2846	**0.2139**
		SNR	35.6968	**39.1685**		SNR	50.9160	**53.3946**
00000267_000	131072	PSNR	40.4658	40.4079	524288	PSNR	43.7691	43.7527
		SSIM	0.4721	0.4711		SSIM	0.6649	0.6641
		PRD	3.2837	**1.4536**		PRD	0.5564	**0.3864**
		SNR	26.6728	**36.7512**		SNR	45.0926	**48.2594**
	262144	PSNR	42.0366	41.7918	798720	PSNR	45.0552	45.0349
		SSIM	0.5515	0.5502		SSIM	0.7298	0.7293
		PRD	1.6412	**0.8136**		PRD	0.2846	**0.2429**
		SNR	35.6968	**42.0041**		SNR	50.9160	**52.2900**

1

Table 1 Sequel

Medical image	Number of bits	Metric	Separated JPEG-2000 / SPIHT	Proposed multimodal scheme	Number of bits	Metric	Separated JPEG-2000 / SPIHT	Proposed multimodal scheme
00005_006	131072	PSNR	41.0859	41.0414	524288	PSNR	44.9093	44.8817
		SSIM	0.5527	0.5518		SSIM	0.7259	0.7246
		PRD	3.2837	**1.4536**		PRD	0.5564	**0.3842**
		SNR	26.6728	**36.7512**		SNR	45.0926	**48.3090**
	262144	PSNR	42.9700	42.9251	798720	PSNR	46.3008	46.2831
		SSIM	0.6304	0.6285		SSIM	0.7744	0.7741
		PRD	1.6412	**0.8136**		PRD	0.2846	**0.2356**
		SNR	35.6968	**41.7918**		SNR	50.9160	**52.5574**
000010_000	131072	PSNR	40.7453	40.6755	524288	PSNR	44.3723	44.3512
		SSIM	0.5296	0.5282		SSIM	0.7065	0.7051
		PRD	3.2837	**1.4536**		PRD	0.5564	**0.3667**
		SNR	26.6728	**36.7512**		SNR	45.0926	**48.7146**
	262144	PSNR	42.4677	42.4438	798720	PSNR	45.7353	45.7060
		SSIM	0.6102	0.6091		SSIM	0.7698	0.7694
		PRD	1.6412	**1.1005**		PRD	0.2846	**0.2356**
		SNR	35.6968	**39.1685**		SNR	50.9160	**52.5574**
000020_001	131072	PSNR	39.9556	39.9122	524288	PSNR	43.5327	43.5163
		SSIM	0.5330	0.5317		SSIM	0.7122	0.7118
		PRD	3.2837	**2.6917**		PRD	0.5564	**0.3924**
		SNR	26.6728	**31.3995**		SNR	45.0926	**48.1261**
	262144	PSNR	41.6605	41.6314	798720	PSNR	44.9359	44.9214
		SSIM	0.6113	0.6099		SSIM	0.7811	0.7808
		PRD	1.6412	**0.8079**		PRD	0.2846	**0.2653**
		SNR	35.6968	**41.8527**		SNR	50.9160	**51.5256**
0001311_000	131072	PSNR	41.3406	41.2611	524288	PSNR	45.3246	45.2871
		SSIM	0.5877	0.5857		SSIM	0.7532	0.7516
		PRD	3.2837	**1.4536**		PRD	0.5564	**0.4008**
		SNR	26.6728	**36.7512**		SNR	45.0926	**47.9411**
	262144	PSNR	43.2136	43.1942	798720	PSNR	46.8660	46.8635
		SSIM	0.6644	0.6636		SSIM	0.7952	0.7951
		PRD	1.6412	**1.1005**		PRD	0.2846	**0.2653**
		SNR	35.6968	**39.1685**		SNR	50.9160	**51.5256**
00001286_ 006	131072	PSNR	41.596	41.5085	524288	PSNR	45.230	45.1769
		SSIM	0.5229	0.5203		SSIM	0.7228	0.7227
		PRD	3.2837	**1.4480**		PRD	0.5564	**0.3792**
		SNR	26.6728	**36.7847**		SNR	45.0926	**48.4224**
	262144	PSNR	43.370	43.3128	798720	PSNR	46.712	46.6217
		SSIM	0.6041	0.6035		SSIM	0.7699	0.7696
		PRD	1.6412	**0.8136**		PRD	0.2846	**0.2541**
		SNR	35.6968	**41.7918**		SNR	50.9160	**51.9015**

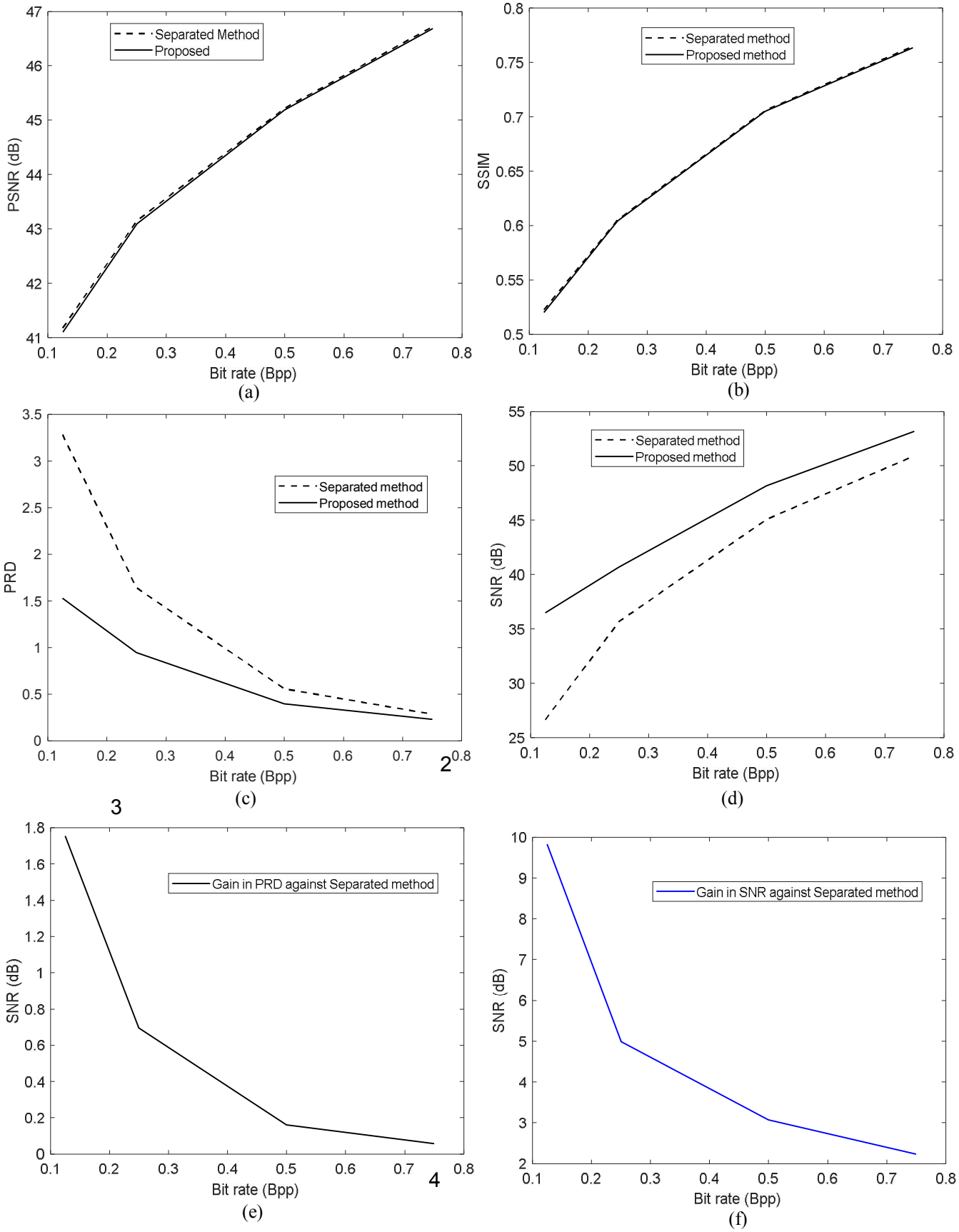

Fig. 4 Performance comparison between the proposed multimodal scheme and the separate method in terms of: (a) Average PSNR. (b) Average SSIM. (c) Average PRD. (d) Average SNR. (e) Average gain in PRD. (f) Average gain in SNR

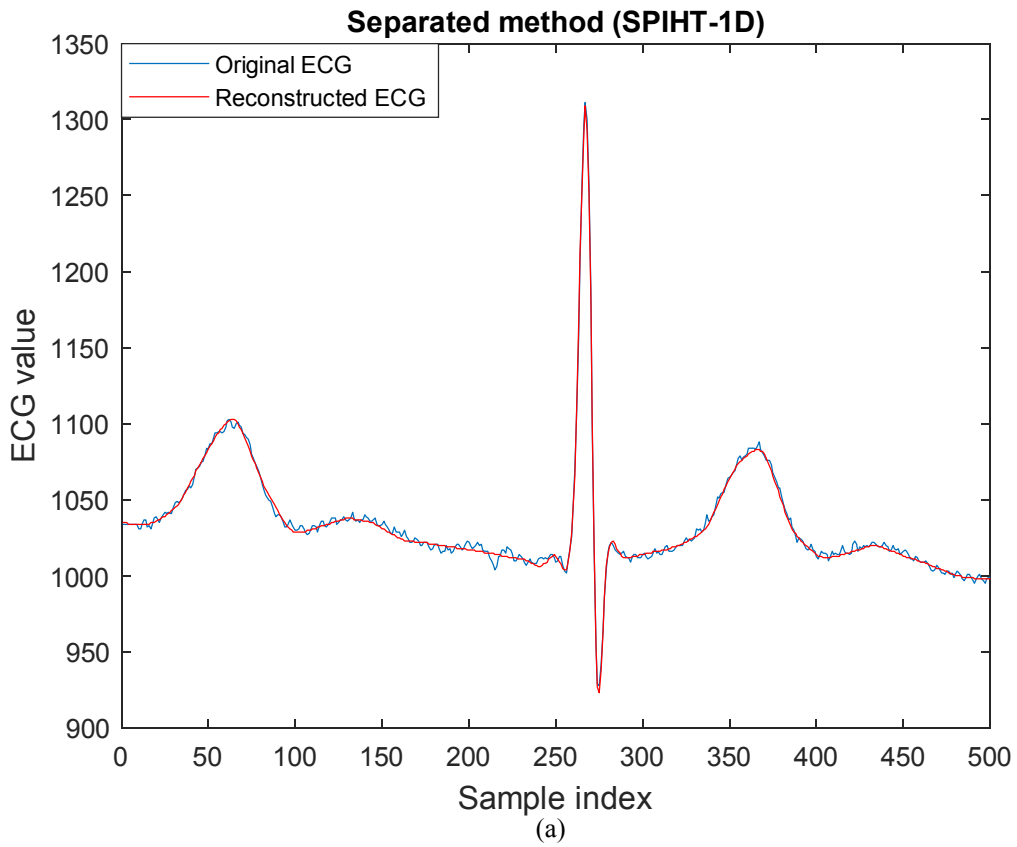

(a)

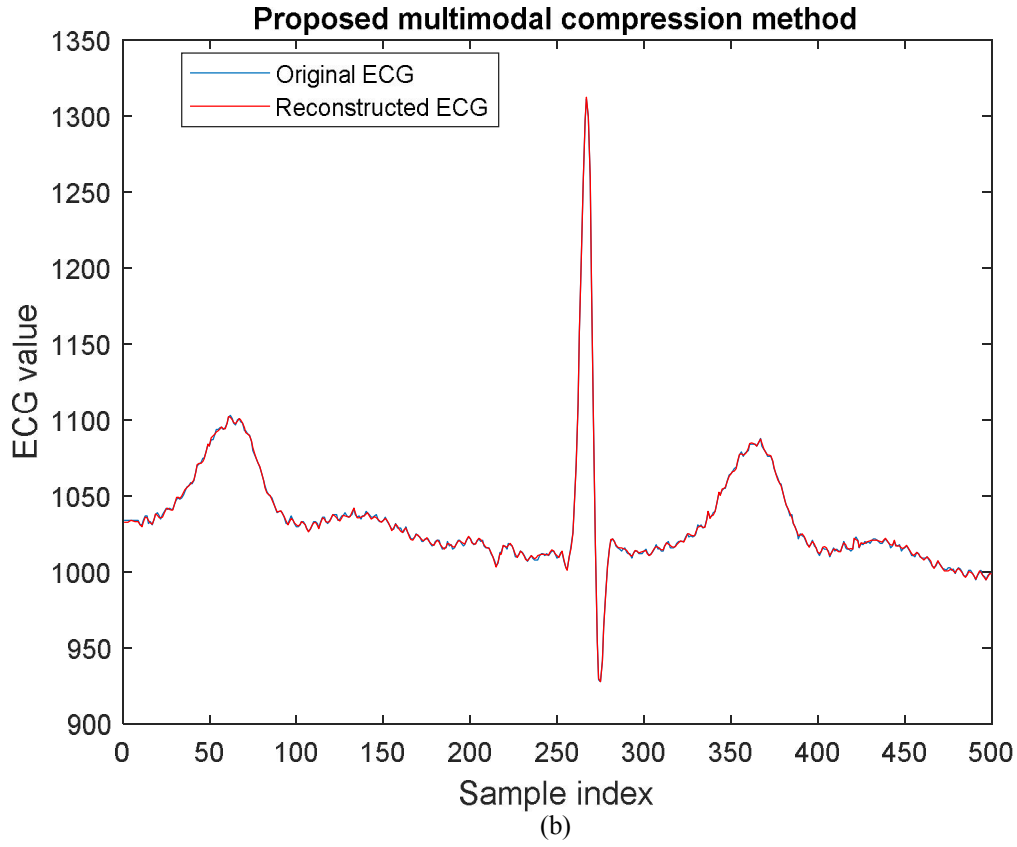

(b)

Fig. 5 Subjective assessment of the proposed multimodal compression method and the separated method (SPIHT-1D) at 798720 bits for the ECG signal (record 103b). (a) Compression with SPIHT-1D of ECG signal: PRD=0.2846, SNR=50.9160 dB. (b) Compression with the proposed method of ECG signal inserted in the medical image 000271_001: PRD=0.08, SNR=61.0953 dB. The gain is up to 10 dB

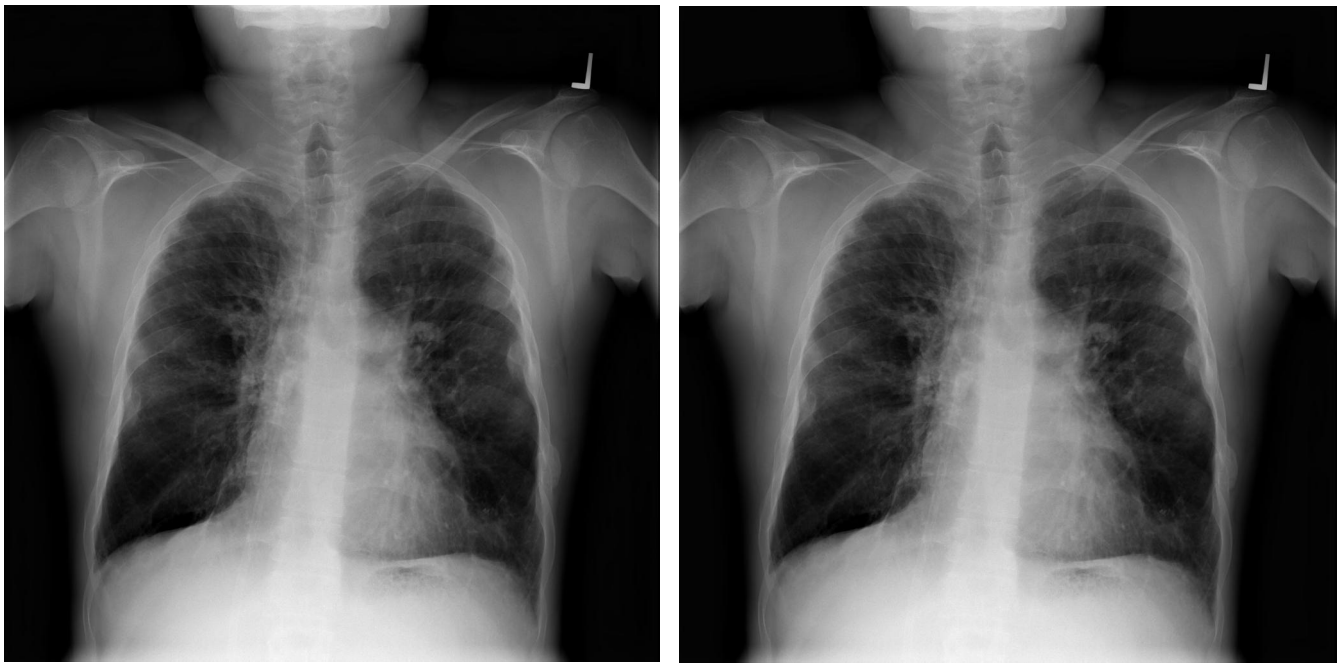

(a) (b)

Fig. 6 Subjective evaluation of the proposed multimodal compression method and the separated method (JPEG-2000) at 798720 bits for the medical image 00001285_000. (a) Compression with JPEG-2000: PSNR=46.699 dB, SSIM=0.7631. (b) Compression of the image along with the ECG signal with the proposed multimodal method: PSNR=46.673 dB., SSIM=0.7622. Both methods have very similar values of PSNR and SSIM. However, the PRD values with the proposed scheme are much lower.

Table 2 Performance compression comparison of the proposed scheme with different multimodal compression methods

Medical image	Bit rate	Metric	Method In [4]	Method In [17]	Method In [6]	Proposed	Bit rate	Metric	Method In [4]	Method In [17]	Method In [6]	Proposed
XR2DLung 10	0.25	PSNR	38.2461	41.913	43.760	43.689	0.75	PSNR	40.0194	46.894	47.118	47.396
		SSIM	0.5023	0.4984	0.5674	0.5604		SSIM	0.6763	0.7077	0.7213	0.7195
		PRD	1.5912	1.190	0.276	**0.246**		PRD	1.2778	0.807	0.223	**0.205**
		SNR	35.9652	38.489	51.166	**52.168**		SNR	37.8705	41.858	53.034	**53.752**
	0.5	PSNR	39.5010	45.014	45.978	46.071	1	PSNR	40.2308	48.039	48.131	48.493
		SSIM	0.6101	0.6168	0.6673	0.6600		SSIM	0.7362	0.7609	0.7609	0.7738
		PRD	1.0954	0.504	0.229	**0.204**		PRD	1.7779	1.42	0.230	**0.188**
		SNR	39.2083	45.954	52.812	**53.821**		SNR	35.0021	36.954	52.768	**54.521**
MR3DBrain 100001	0.25	PSNR	39.9453	40.619	40.650	40.793	0.75	PSNR	48.5750	48.876	48.793	49.159
		SSIM	0.3561	0.3422	0.3457	0.3500		SSIM	0.7156	0.7158	0.7338	0.7336
		PRD	2.5114	3.907	0.395	**0.385**		PRD	1.9167	1.660	0.224	**0.204**
		SNR	32.0016	28.164	48.065	**48.300**		SNR	34.3489	35.596	52.986	**53.821**
	0.5	PSNR	45.7319	45.742	45.938	46.140	1	PSNR	51.1077	51.551	51.099	51.803
		SSIM	0.5464	0.5402	0.5540	0.5607		SSIM	0.8228	0.8291	0.8393	0.8446
		PRD	2.5415	2.6409	0.276	0.277		PRD	1.3271	1.0186	0.202	**0.169**
		SNR	31.8981	31.565	51.166	51.141		SNR	37.5418	39.840	53.892	**55.442**
IM001	0.25	PSNR	41.1053	42.166	42.169	42.286	0.75	PSNR	46.4677	46.966	47.007	47.380
		SSIM	0.5633	0.5873	0.6011	0.5944		SSIM	0.7811	0.7947	0.8043	0.7992
		PRD	2.9099	3.923	0.373	**0.371**		PRD	1.6521	1.358	0.224	**0.204**
		SNR	30.7225	28.127	48.567	**48.605**		SNR	35.6394	37.340	52.986	**53.821**
	0.5	PSNR	44.5964	45.517	45.336	45.430	1	PSNR	47.9395	48.264	48.437	48.822
		SSIM	0.7161	0.7343	0.7363	0.7366		SSIM	0.8385	0.8396	0.8466	0.8546
		PRD	2.2707	2.792	0.274	**0.248**		PRD	1.8093	1.507	0.239	**0.219**
		SNR	32.8770	31.081	51.258	**52.119**		SNR	34.8500	36.440	52.429	**53.203**
IM005	0.25	PSNR	39.8604	41.634	41.501	41.594	0.75	PSNR	45.6882	46.866	46.789	47.187
		SSIM	0.5273	0.5864	0.5926	0.5903		SSIM	0.8054	0.8286	0.8319	0.8324
		PRD	3.6279	3.1840	0.338	**0.315**		PRD	1.9689	1.661	0.175	0.175
		SNR	28.8070	29.940	49.422	**50.024**		SNR	34.1154	35.590	55.157	55.118
	0.5	PSNR	43.8432	44.865	45.184	45.364	1	PSNR	46.9360	48.215	48.181	48.589
		SSIM	0.7273	0.7396	0.7705	0.7702		SSIM	0.8576	0.8701	0.8746	0.8762
		PRD	3.2290	2.601	0.27	**0.265**		PRD	1.0545	1.492	0.161	**0.137**
		SNR	29.8186	31.6979	51.374	**51.519**		SNR	39.5392	36.527	55.875	**57.280**
00001311_000	0.25	PSNR	34.5038	39.5789	39.4468	39.5303	0.75	PSNR	35.8847	45.0541	45.2524	45.4762
		SSIM	0.6792	0.7028	0.7040	0.7047		SSIM	0.8001	0.8224	0.8268	0.8307
		PRD	4.9006	3.6865	0.3565	**0.3284**		PRD	2.2172	1.5408	0.2205	**0.2039**
		SNR	26.1950	28.6677	48.9600	**49.6718**		SNR	33.0838	36.2452	53.1305	**53.8101**
	0.5	PSNR	35.5790	43.3311	43.1476	43.3922	1	PSNR	36.1015	46.4246	46.4821	47.1116
		SSIM	0.7639	0.7925	0.7931	0.7963		SSIM	0.8251	0.8447	0.8530	0.8537
		PRD	3.3277	2.8138	0.2751	**0.2514**		PRD	1.8408	1.0556	0.1967	**0.1883**
		SNR	29.5570	31.0141	51.2103	**51.9920**		SNR	34.7001	39.5299	54.1247	**54.5030**

2

Table 2 Sequel

1

Medical image	Bit rate	Metric	Method In [4]	Method In [17]	Method In [6]	Proposed	Bit rate	Metric	Method In [4]	Method In [17]	Method In [6]	Proposed
I27	0.25	PSNR	32.1080	32.4628	32.538	32.595	0.75	PSNR	36.0403	36.7314	36.844	37.305
		SSIM	0.2686	0.2748	0.2696	0.2675		SSIM	0.5311	0.5376	0.5381	0.5430
		PRD	4.7174	2.9542	0.278	**0.276**		PRD	4.2639	3.1899	0.292	**0.269**
		SNR	26.5259	30.5913	51.122	**51.194**		SNR	27.4038	29.9244	50.679	**51.404**
	0.5	PSNR	34.5203	35.1358	35.121	35.399	1	PSNR	36.7455	37.5954	37.673	38.278
		SSIM	0.3986	0.4038	0.4024	**0.3979**		SSIM	0.5918	0.6069	0.6099	0.6001
		PRD	2.5138	2.9954	0.198	**0.196**		PRD	2.4572	2.4467	0.224	**0.215**
		SNR	31.9934	30.4710	54.076	54.133		SNR	32.1910	32.2283	52.982	**53.354**
Endoscope1	0.25	PSNR	38.3522	39.4476	39.603	39.743	0.75	PSNR	44.6076	46.6211	46.640	46.846
		SSIM	0.5303	0.5787	0.6018	0.6019		SSIM	0.8848	0.9207	0.9206	0.9215
		PRD	3.9988	2.5645	0.270	**0.267**		PRD	1.2741	1.2830	0.175	**0.175**
		SNR	27.9613	31.8198	51.364	**51.466**		SNR	37.8957	37.8355	55.157	**55.128**
	0.5	PSNR	41.7944	43.8148	43.698	44.041	1	PSNR	46.4602	48.4772	48.423	48.717
		SSIM	0.7590	0.8470	0.8491	0.8551		SSIM	0.9239	0.9457	0.9498	0.9490
		PRD	2.0605	2.0590	0.237	**0.232**		PRD	0.9029	0.9243	0.164	**0.130**
		SNR	33.7205	33.7269	52.516	**52.708**		SNR	40.8873	40.6835	55.703	**57.694**
Eye2	0.25	PSNR	44.3854	46.0094	45.903	45.936	0.75	PSNR	46.7380	48.3654	48.364	48.645
		SSIM	0.3473	0.4194	0.4254	0.4178		SSIM	0.6805	0.6885	0.7195	0.7053
		PRD	3.2868	3.2801	0.228	**0.212**		PRD	0.5167	0.4719	0.092	**0.085**
		SNR	29.6644	29.6822	52.835	**53.467**		SNR	45.7357	46.5237	60.742	**61.412**
	0.5	PSNR	45.8007	47.5901	47.434	47.785	1	PSNR	47.6922	50.0742	49.531	50.053
		SSIM	0.5477	0.6135	0.6295	0.6321		SSIM	0.7650	0.7957	0.8025	0.7973
		PRD	1.6368	1.6112	0.186	**0.171**		PRD	1.1299	1.3524	0.123	**0.108**
		SNR	35.7199	35.8571	54.625	**55.323**		SNR	38.9391	37.3778	58.219	**59.333**
00000010_000	0.25	PSNR	37.2947	39.3597	39.311	39.473	0.75	PSNR	41.1192	44.9134	44.903	45.066
		SSIM	0.5880	0.6363	0.6374	0.6396		SSIM	0.7404	0.7651	0.7673	0.7712
		PRD	2.9633	2.9126	0.324	**0.323**		PRD	2.0198	2.0301	0.247	**0.205**
		SNR	30.5644	30.7144	49.802	**49.828**		SNR	33.8939	33.8494	52.160	**53.762**
	0.5	PSNR	39.7151	42.5948	42.656	42.893	1	PSNR	41.9480	46.3566	46.203	46.622
		SSIM	0.6833	0.7181	0.7270	0.7289		SSIM	0.7808	0.7951	0.7954	0.8007
		PRD	1.9790	1.9945	0.237	**0.232**		PRD	1.8764	1.6613	0.175	**0.172**
		SNR	34.0710	34.0035	52.491	**52.708**		SNR	34.5335	35.5909	55.157	**55.285**
00000003_006	0.25	PSNR	37.8184	40.0527	39.917	39.961	0.75	PSNR	41.3610	45.2775	45.398	45.419
		SSIM	0.6003	0.6432	0.6426	0.6430		SSIM	0.7474	0.7749	0.7782	0.7797
		PRD	3.8315	3.6404	0.270	**0.267**		PRD	2.1986	2.2332	0.199	**0.175**
		SNR	28.3326	28.7769	51.364	**51.466**		SNR	33.1569	33.0213	54.04	**55.139**
	0.5	PSNR	40.2594	43.2886	43.352	43.492	1	PSNR	41.8555	46.5244	46.513	46.987
		SSIM	0.7000	0.7335	0.7372	0.7366		SSIM	0.7747	0.8048	0.8031	0.8042
		PRD	2.1994	2.1982	0.219	**0.215**		PRD	1.3101	1.3337	0.183	**0.171**
		SNR	33.1538	33.1588	53.186	**53.354**		SNR	37.6540	37.4991	54.772	**55.323**

shows slight improvements in terms of PRD, while the method [6] significantly outperforms the methods [4] [17] . On the other hand, the method in [17] delivers superior performance in terms of image quality when compared to [4] while maintaining good signal quality at the decompression stage. Overall, the proposed scheme seems to reach the best trade-off between image and signal quality.

4.3 Complexity analysis

To explore the complexity of three multimodal methods, the average running time is measured. The programs were written in Matlab and tested in the same computing environment using the same computing platform (Dell Precision , Processor 2.7 GHz Intel Core i7-3740 QM, Memory 16 GB). The results obtained are reported in Table 3. On average, the proposed method performs the multimodal compression faster than its competitors. This is mainly due to the simple and yet efficient ECG insertion method proposed in the wavelet domain.

Table 3 Comparison of coding time (in seconds) of three multimodal compression methods

	Medical image					
Method	00000010_000	00003_006	1311_000	XR2DLung10	MR3DBrain 100001	Average
[4]	0.7635	0.7700	0.7669	0.7806	0.7778	0.7718
[6]	1.1028	1.1039	1.1003	1.1004	1.0920	1.0999
Proposed	0.6365	0.6425	0.6396	0.6318	0.6364	0.6374

5. Conclusion

An alternative technique is proposed to compress jointly and simultaneously a medical image and electrocardiogram signals, using only the standard JPEG-2000.In comparison with the conventional technique based on the use of two codecs (JPEG-2000 for image compression and SPIHT-1D for ECG compression) the proposed technique reduces the computational complexity and improves the signal quality while exhibiting good image quality. Comparative results with existing unsupervised multimodal compression techniques, using objective evaluation tests, indicate that our multimodal compression scheme delivers superior performance for both reconstructed image and signal.

References

1 Salomon D (2011) Data compression: the complete reference," 4th ed. Springer

2 Sayood k (2017) Introduction to data compression. Morgan Kaufmann. Elsevier

3 Al-Fahoum A (2006) Quality assessment of ECG compression techniques using a wavelet-based diagnostic measure IEEE Transactions on Information Technology in Biomedicine 10:182–191

4 Nait-Ali A, Zeybek E H, Drouot X (2009) Introduction to multimodal compression of biomedical data. In: Nait-Ali A (ed) Advanced biosignal processing: book. Springer, pp 353–375

5 Boubchir L, Brahimi T, Fournier R, Nait-Ali A(2012) A novel multimodal compression scheme based on a spiral insertion function in the wavelet domain. In:The11th international conference on information sciences, signal process and their applications(ISSPA), pp97–102

6 Brahimi T., Boubchir L., Fournier R., Nait-Ali A. (2017) An improved multimodal signal image compression scheme with application to natural images and biomedical data. Multimedia Tools Appl 76(15) 16783–16805

7 Shapiro J. M. (1993) Embedded image coding using zerotrees of wavelet coefficients *IEEE Transactions on Signal Processing* 41(12): 3445–3462

8 Said A, Pearlman WA. (1996) A new, fast, and efficient image codec based on set partitioning in hierarchical trees IEEE Transactions on Circuits and Systems for Video Technology 6(3): 243–250

9 Pearlman W A, Islam A, Nagaraj N, Said A (2004) Efficient, low-complexity image coding with a set-partitioning embedded block coder. IEEE Transactions on Circuits and Systems for Video Technology, 14(11): 1219–1235

10 Taubman D (2000) High Performance Scalable Image Compression with EBCOT. IEEE Transactions on Image Processing, 9(7): 1158–1170

11 ITU. (2012) JPEG XR image coding system reference software.[Online]. Available: http://www.itu.int/rec/T-REC-T.835-201201-I/en

12 Lu Z, Kim D Y, Pearlman W A (2000) Wavelet compression of ECG signals by the set partitioning in hierarchical trees algorithm. IEEE Transactions on Biomedical Engineering 47(7): 849–856

13 Padhy S, Sharma L N, Dandapat S (2016) Multilead ECG data compression using SVD in multiresolution domain. Biomedical Signal Processing and Control, 23:10–18

14 Wang X, Chen Z, Luo J, Meng J, Xu Y (2016) ECG compression based on combining of EMD and wavelet transform. Electronics Letters, 52(19):1588–1590

15 MA J, Zhang T T, Dong M (2015) A novel ECG data compression method using adaptive fourier decomposition with security guarantee in e-health applications. IEEE Journal of Biomedical and Health Informatics19(3): 86–994

16 Grossi G, Lanzarotti R, Lin J (2015) High-rate compression of ECG signals by an accuracy-driven sparsity model relying on natural basis. *Digital Signal Processing*, 45: 96–106

17 Zeybek E H, Nait-Ali A, Christian O, Ouled-Zaid A (2007) A novel scheme for joint multi-channel ECG-ultrasound image compression, Proceedings of the 29th Annual International Conference of the IEEE Engineering in Medicine and Biology Society (EMBS): 713–716

18 Zeybek E H, Fournier R, Nait-Ali A (2012) Multimodal compression applied to biomedical data. Journal of Biomedical Science and Engineering 5: 755–761

19 Christopoulos C, Skodras A, Ebrahimi T (2000) The JPEG-2000 Still Image Coding System: An Overview. IEEE Transactions on. Consumer Electronics 46(4): 1103–1127

20 Skodras A, Christopoulos C, Ebrahimi T (2001) The JPEG 2000 Still Image Compression Standard. IEEE Signal Processing Magazine 18(5): 36–58

21 Marcellin M W, Gormish M J, Bilgin A, Boliek M P (2000) An Overview of JPEG-2000. Proceedings of .Data Compression Conference, 523–541

22 Fournier R, Naït-Ali A (2012) Multimodal Compression Using JPEG 2000: Supervised Insertion Approach. In:Ouahabi A(ed) Signal and image multiresolution analysis:book.Willey,pp225–243

23 Mallat S (2008) *A Wavelet Tour of Signal Processing*. 3rd ed. Academic press

24 Ghanbari M (2011) Standard Codecs Image compression to advanced video coding. 3rd ed. IEE, London, UK

25 Khelifi F,Bouridane A, Kurugollu F (2008) Joined spectral trees for scalable SPIHT-based multispectral image compression. IEEE Transactions on Multimedia, 10(3): 316–329

26 Bouridane A, Khelifi F, Amira A, et *al.* (2004) A very low bit-rate embedded color image coding with SPIHT. Proceedings of Acoustics, Speech, and Signal Processing, 2004. (ICASSP'04). IEEE International Conference on. IEEE, p. iii–689

27 Brahimi T, Laouir F, Kechacha N (2008) An efficient wavelet-based image coder. In :The 3rd , IEEE international conference on information and communication technologies : from theory to applications (ICTTA), pp1–4

28 Brahimi T, Laouir F, Boubchir L, Ali-Chérif A (2017) An improved wavelet-based image coder for embedded greyscale and colour image compression, AEU-International Journal of Electronics and Communications, 73:183–192

29 Pearlman W A (2013).Wavelet image compression. Synthesis Lectures on Image, Video, and Multimedia Processing, 8(1):1–90

30 Usevitch B E (2001) A Tutorial on modern lossy wavelet image compression: foundations of JPEG2000. Signal Processing Magazine,18 (5): 22–35

31 Gargour C, Gabrea M, Ramanchandran V, Lina J-M (2009) A short introduction to wavelets and their applications IEEE Circuits and Systems Magazine 9(2): 57–68

32 Pearlman W A, Said A (2011) Digital signal compression : principle and practice. Cambridge University Press,United Kingdom

33 Khelifi F, Kurugollu F, Bouridane A (2008) SPECK-based lossless multispectral image coding. IEEE Signal Processing Letters 15: 69–72

34 Daubechies I, Sweldens W (1998) Factoring wavelet transforms into lifting steps. J. Fourier Anal. Appl., 4 247–269

35 Calderbank A R, Daubechies I, Sweldens W, Yeo B L (1998) Wavelet transforms that map integers to integers. Applied and Computational Harmonic Analysis 5(3): 332–369

36 Adams M D, Kossentni F (2000) Reversible integer-to-integer wavelet transforms for image compression: performance evaluation and analysis. IEEE Transactions on Image Processing, 9(6): 1010–1024

37 Brahimi T, Khelifi F, Melit A, Boutana D (2008) Efficient lossless colour image coding with modified SPIHT. Mediterranean Journal of Electronics and Communications 4(4): 148–153

38 Brahimi T, Melit A, Khelifi F (2009) An improved SPIHT algorithm for lossless image coding. Digital Signal Processing 19(2): 220–228

39 Weinberger M J, Seroussi G, Sapiro.G (1998). The LOCO-I Lossless Compression Algorithm: Principles and Standardization into JPEG-LS. Technical Report HPL-98–193, Hewlett-Packard Laboratory

40 Weinberger M J, Seroussi G, Sapiro.G (2000) The LOCO-I lossless image compression algorithm: Principles and standardization into JPEG-LS. IEEE Transactions on Image processing, 9(8): 1309–1324

41 Open-Access Medical Image Repositories: http://www.aylward.org/notes/open-access-medical-image-repositories

42 Zhou, W., Bovik A. C., Sheikh H. R., and Simoncelli E. P (2004). Image Qualifty Assessment: From Error Visibility to Structural Similarity. IEEE Transactions on Image Processing, 13(4): 600–612.

Open-Access Medical Image Repositories: